

Supporting Information

Facile aqueous synthesis of β -AgI nanoplates as efficient visible-light-responsive photocatalyst

Wen Jiang^a, Changhua An^{*a, b}, Junxue Liu^b, Shutao Wang^b, Lianming Zhao^b, Wenyue Guo, ^{*a, b}
and Jinxiang Liu^c

^a State Key Laboratory of Heavy Oil Processing, College of Chemical Engineering, China University of Petroleum, Qingdao 266580, China P. R.
Fax: (+86) 532-86981787; Tel: 0532-86983415;

E-mail: anchh@upc.edu.cn

^b Department of Materials Physics and Chemistry, College of Science, China University of Petroleum, Qingdao 266580, China P. R.

E-mail: wgyuo@upc.edu.cn

^c School of Chemistry and Chemical Engineering, Shandong University, Jinan 250100, China P. R.

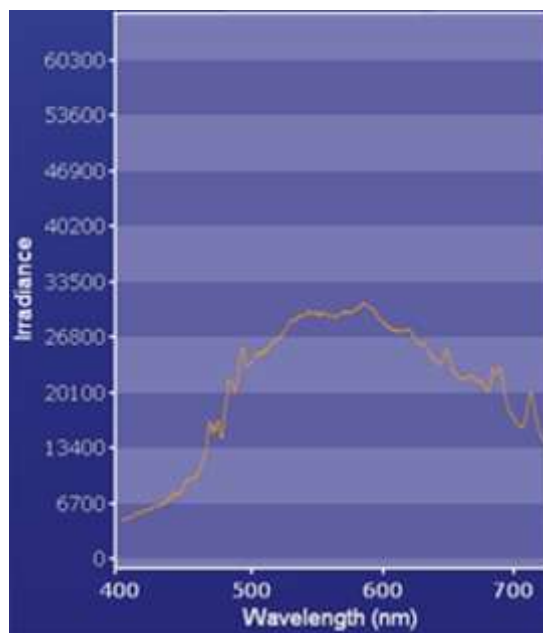


Figure S1

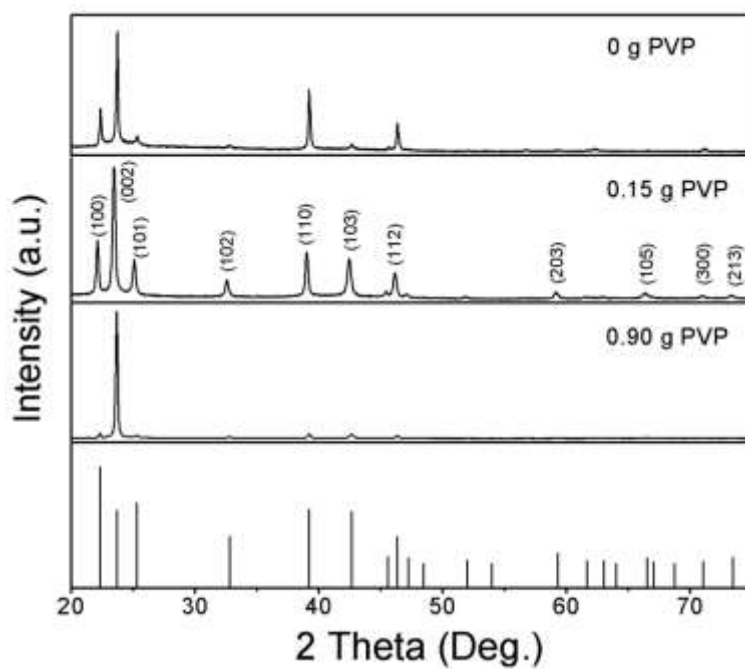


Figure S2. XRD patterns of AgI nanoparticles prepared with different amount of PVP and the standard diffraction of AgI powder highlighted by sticks.

| PVP / g | Color Change |
|---------|---|
| 0 |  0 min, 0.12 min, 2.5 min, 110 min |
| 0.15 |  0 min, 27 min, 75 min, 110 min |
| 0.375 |  0 min, 27 min, 75 min, 110 min |
| 0.9 |  0 min, 27 min, 75 min, 110 min |

Figure S3. The color changes in the reaction mixture with PVP varied from 0 g to 0.9 g at different reaction times.

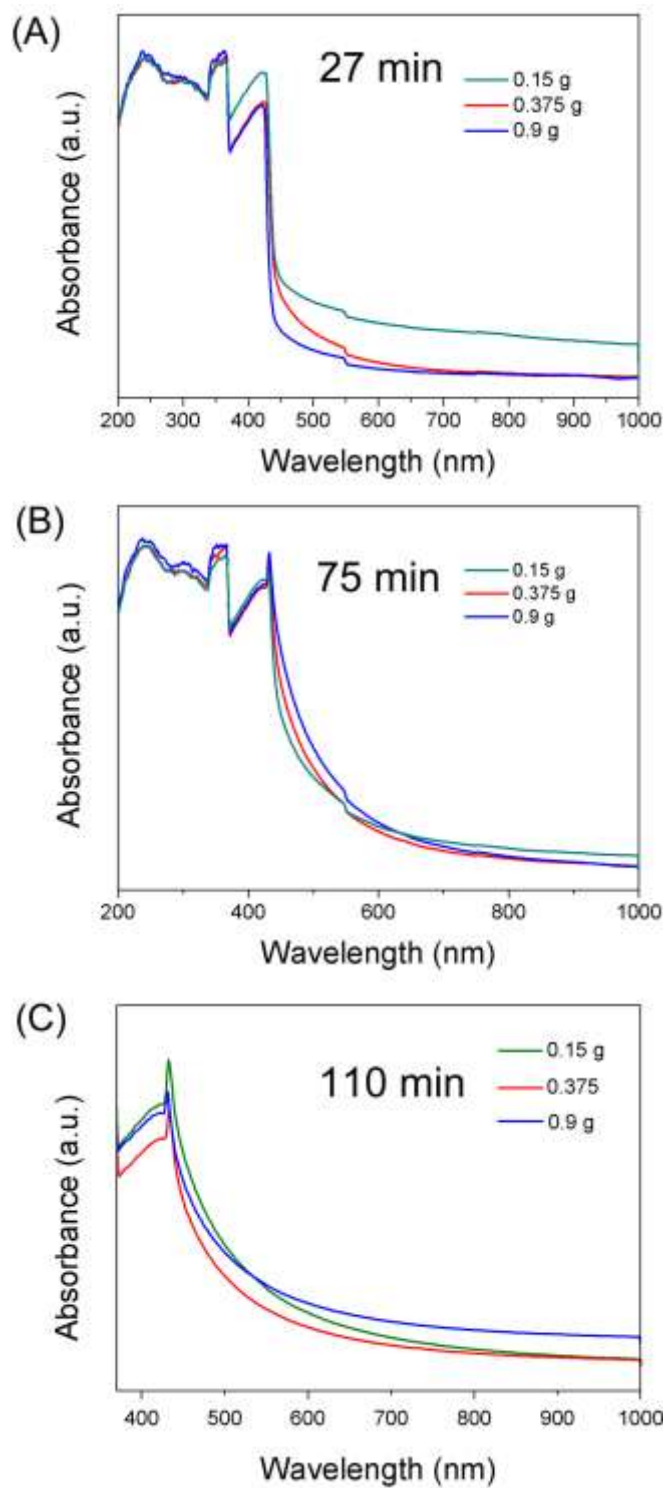


Figure S4. UV-*vis* spectra of the obtained samples with various amount of PVP at different reaction times (A) 27 min, (B) 75 min, and (C) 110 min.

In the reaction process, aliquots of 2 mL of solution at different reaction times were taken out to be measured with UV-*vis* spectroscopy. Figure S2 shows that PVP have great influence for the existing state of iodide ions, which is important for the growth of AgI nanoparticles. Without PVP, the KI solution (reaction time denoted as 0 min) is colorless and transparent, while it turns out to be yellow once PVP introduced. What's more, only 0.17 min was taken for the reaction mixture to become turbid without PVP. Meanwhile, the reaction involved PVP need 27 min to complete the color change. With the amount of PVP increased, the samples taken at 27 min become clearer sequentially, meaning PVP may depress the nucleation and growth of small AgI crystals. The suspensions obtained at 75 min have no obvious difference in terms of turbidity. However, the samples at 110 min displayed abnormal tendency, where the turbidity is following the order of nanoparticles synthesized with 0.15 g, 0.9 g and 0.375g of PVP. To further investigate the growth process, UV-*vis* spectra of the samples, as shown in Figure S3, were also measured. Figure S3A shows nanoplates synthesized with 0.15 g PVP exhibits stronger characteristic absorption than nanoplates synthesized with 0.375 g and 0.9 g PVP. Coinciding with the colors' feature, characteristic absorption peak of the latter nanoplates are somewhat overlapped. The results indicate that the sample synthesized with 0.15 g PVP contains the greatest amount of AgI seeds after the reaction proceeded 27 min. Figure S3B shows that the concentration of AgI nanoparticles in 3 reaction systems are almost the same, indicating that the growth of AgI nanoplates involved 0.375 g and 0.9 g PVP is faster than that synthesized with 0.15 g PVP. The tendency shown in Figure S3C matches the color changes in Figure S2. The larger edge length and weaker absorbance of the final product reveals that the reaction with 0.375 g PVP manifests the fastest growth speed.

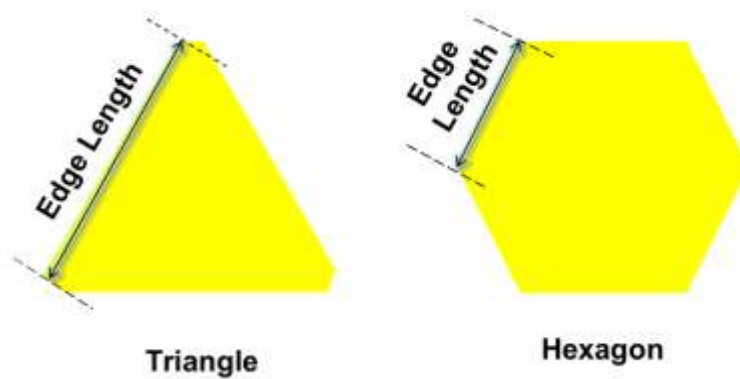


Figure S5. Schematic illustration for the calculation of the edge lengths for the as-synthesized AgI nanoplates.

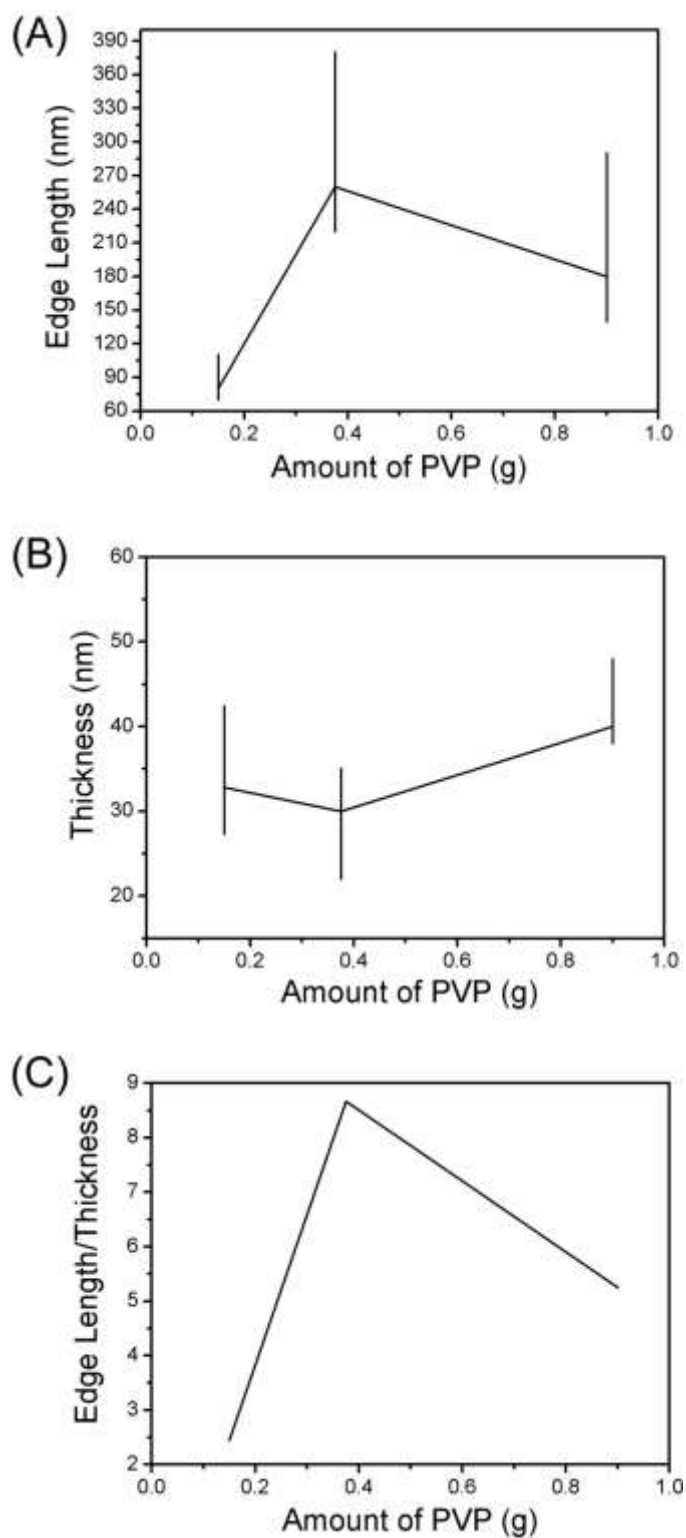


Figure S6. The variation of (A) edge length, (B) thickness and (C) aspect ratio of edge length to thickness of AgI nanoplates with the change of PVP added.

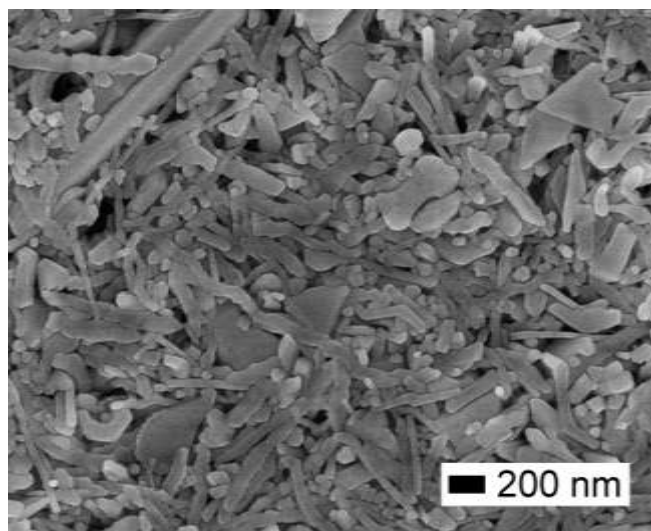


Figure S7 SEM image of the synthesized AgI nanoparticles with 0.05 g PVP.

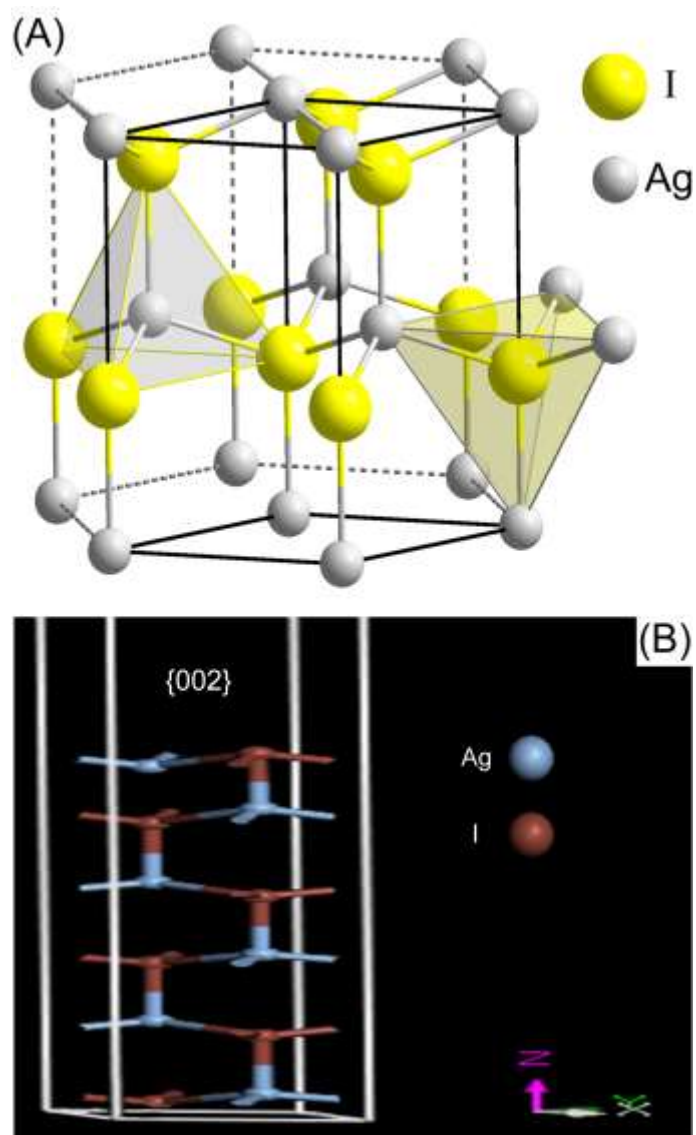


Figure S8. Crystal structure and relaxed geometries for the {002} surface of β -AgI based on a 12 (24)-atom slab model.

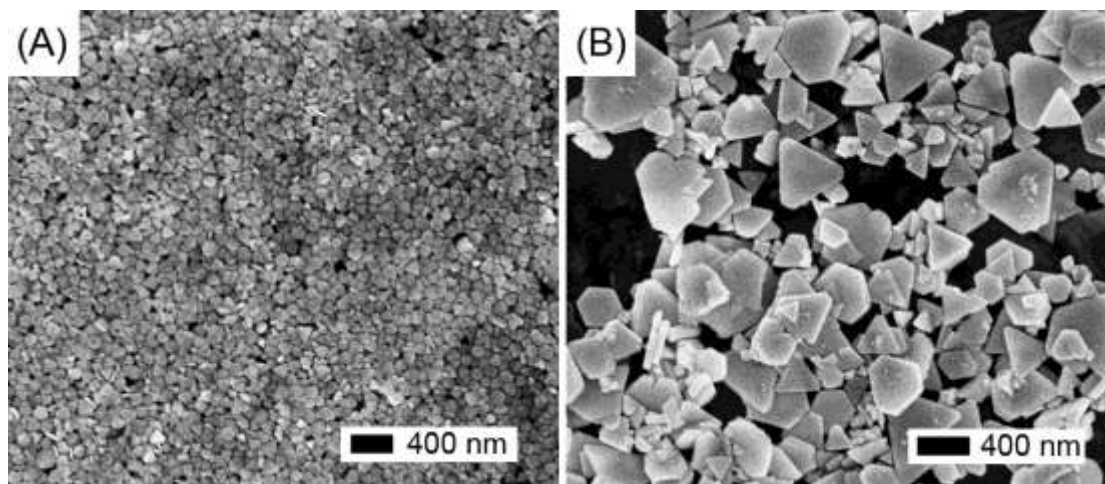


Figure S9. SEM images of AgI nanoplates obtained with different molar ratio of I⁻ to Ag⁺, (A) 1 and (B) 1.5.

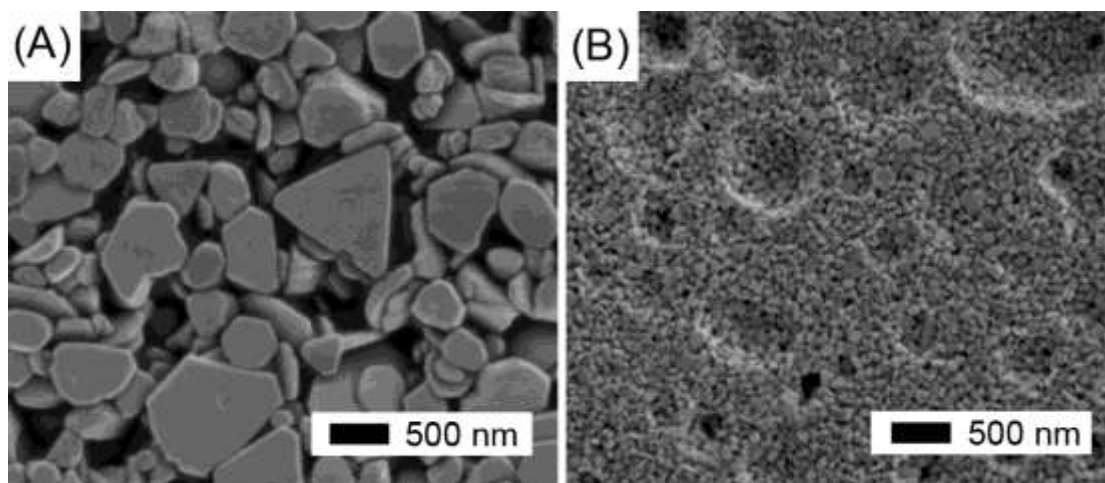


Figure S10. SEM images of as-synthesized products in the solvents of (A) dimethyl sulfoxide and (B) glycerol.

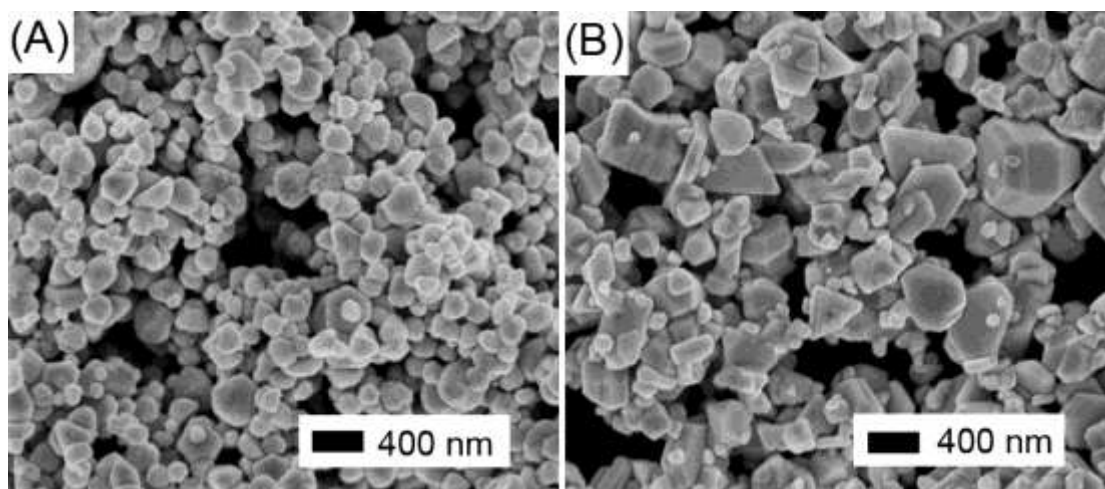


Figure S11. SEM images of AgI nanoparticles prepared with the presence of (A) CTAB and (B) SDBS in aqueous solution.

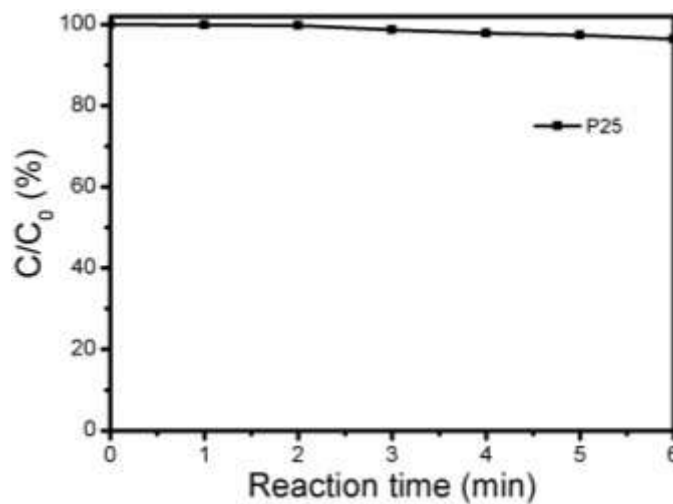


Figure S12. Photodegradation curve of RhB solution catalyzed by P25 with the same condition as AgI sample shown in Figure 6.

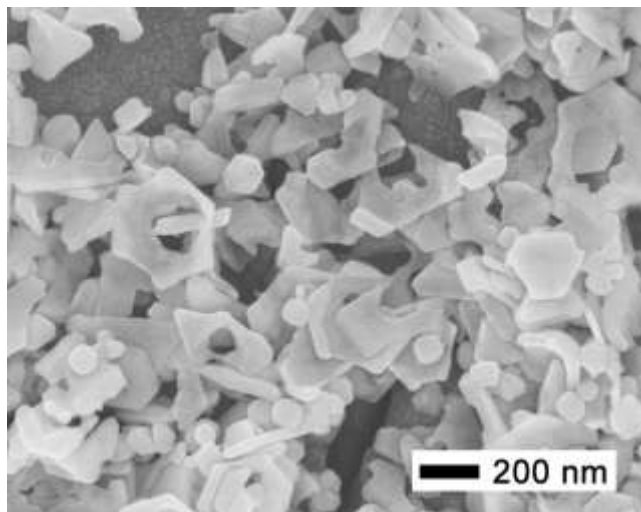


Figure S13. SEM image of AgI nanoplate (synthesized with 0.375 g PVP) after used 10 times for the degradation of RhB solution, showing that the morphology changed from original plate to hollow-plate and collapsed fragments.

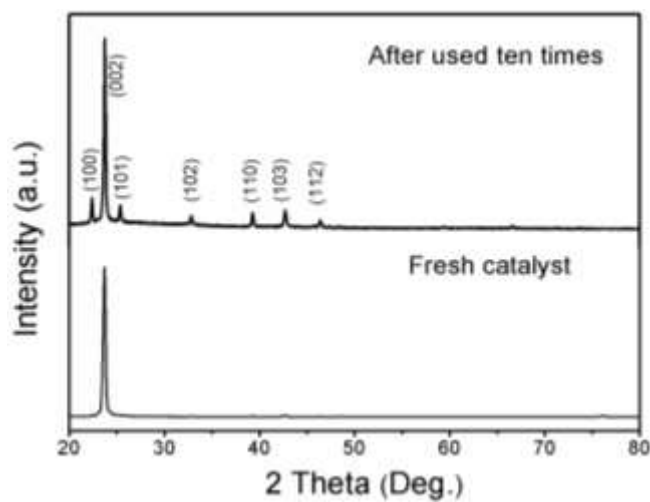


Figure S14. XRD patterns of AgI nanoparticles (synthesized with 0.375 g PVP) before and after photocatalytic degradation of RhB.

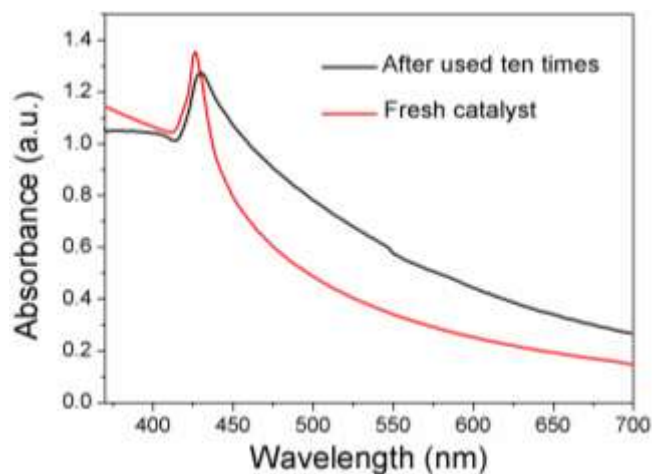


Figure S15. UV-*vis* spectra of AgI nanoparticles (synthesized with 0.375 g PVP) before and after photocatalytic degradation of RhB. It is clearly shown that absorption peak of AgI after photocatalytic reaction exhibits wider absorption than fresh catalyst, which can be attributed to the broad size-distribution of the used AgI particles (as shown in Figure S13).

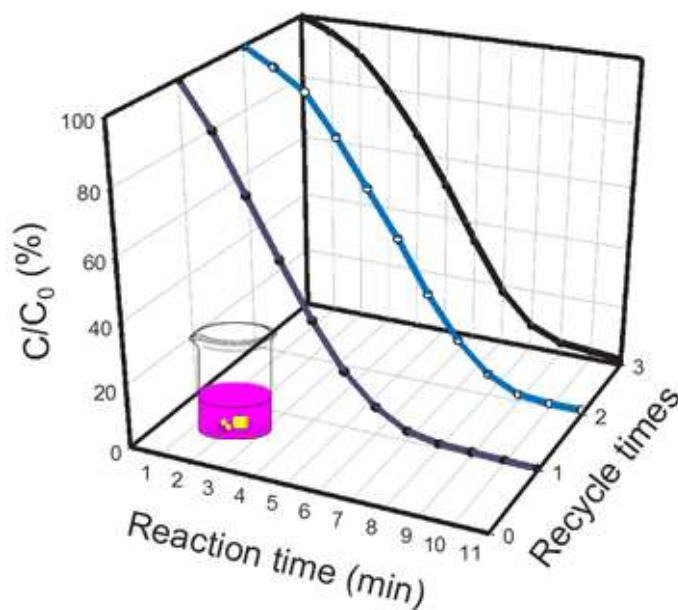


Figure S16. The degradation kinetics of RhB molecules for 3 successive reactions catalyzed by the same batch of AgI nanoparticles shown in Figure 4D under visible light irradiation.

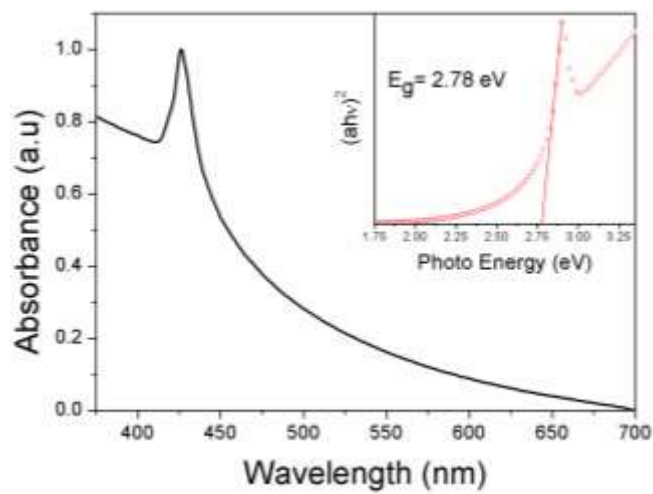


Figure S17. A UV-*vis* absorption spectrum of AgI nanoplates. The inset highlights the bandgap estimation following the spectrum.